J|A|C|S
ARTICLES
Published on Web 12/29/2006

Design of a Functional Membrane Protein by Engineering a Heme-Binding Site in Glycophorin A

Jeanine M. Cordova,[†] Pamela L. Noack,[†] Simon A. Hilcove,[†] James D. Lear,[‡] and Giovanna Ghirlanda*[,†]

Contribution from the Department of Chemistry and Biochemistry, Arizona State University, Tempe, Arizona 85287-1604, and Department of Biochemistry and Biophysics, University of Pennsylvania, Philadelphia, Pennsylvania 19104

Received November 2, 2005; E-mail: gghirlanda@asu.edu

Abstract: We have designed a functional model membrane protein by engineering a bis-Histidine heme-binding site into a natural membrane protein, glycophorin A (GpA), structurally characterized by the dimerization of a single transmembrane helix. Out of the 32 residues comprising the transmembrane helix of GpA, five amino acids were mutated; the resulting protein, ME1, has been characterized in dodecyl phosphocholin (DPC) micelles by UV−vis, CD spectroscopy, gel electrophoresis, and analytical ultracentrifugation. ME1 binds heme with sub-micromolar affinity and maintains the highly helical secondary structure and dimeric oligomerization state of GpA. The ME1−Heme complex exhibits a redox potential of −128 ± 2 mV vs SHE, indicating that the heme resides in a hydrophobic environment and is well shielded from the aqueous phase. Moreover, ME1 catalyzes the hydrogen peroxide dependent oxidation of organic substrates such as TMB (2,2′,5,5′-tetramethyl-benzidine). This protein may provide a useful framework to investigate how the protein matrix tunes the cofactor properties in membrane proteins.

Introduction

De novo designed, water-soluble peptide−heme complexes have long served as model systems for studying how the protein matrix controls the properties and function of the cofactor in natural hemoproteins. Systems of varying structural and functional complexities have been presented over the years,[1−11] with the simplest models consisting of a single heme moiety sandwiched between two short helical peptides[12−19] and ligated by two axial histidine residues. Additional strategies to stabilize these assemblies include the covalent linking of the porphyrin to the peptide chain[16−19] or the preorganization of the peptides via disulfide bonds into hairpins and cyclic systems.[12−15] In both approaches, the free peptide is unfolded but assumes an α-helical structure upon coordination of the porphyrin cofactor.

In contrast to water-soluble model hemoproteins, relatively little work has been done on membrane-soluble systems.[20−24] One attractive feature of membrane proteins is that transmembrane helices are inherently more stable than their water-soluble counterparts of similar length, because the α-helical structure can effectively sequester the polar peptide bonds from the nonpolar environment via intrahelical backbone hydrogen bonds.[25,26] Thus, it should be comparatively easier to design stable transmembrane helical proteins in which folding and binding of heme could be decoupled. However, the interhelical interactions that control the folding of secondary structure

[†] Arizona State University.
[‡] University of Pennsylvania.

(1) Lombardi, A.; Nastri, F.; Pavone, V. *Chem. Rev.* **2001**, *101*, 3165−3189.
(2) Rau, H. K.; DeJonge, N.; Haehnel, W. *Angew. Chem. Int., Ed.* **2000**, *39*, 250−253.
(3) Rau, H. K.; Haehnel, W. *J. Am. Chem. Soc.* **1998**, *120*, 468−476.
(4) Rojas, N. R.; Kamtekar, S.; Simons, C. T.; McLean, J. E.; Vogel, K. M.; Spiro, T. G.; Farid, R. S.; Hecht, M. H. *Protein Sci.* **1997**, *6*, 2512−2524.
(5) Reedy, C. J.; Gibney, B. R. *Chem. Rev.* **2004**, *104*, 617−649.
(6) Moffet, D. A.; Hecht, M. H. *Chem. Rev.* **2001**, *101*, 3191−3203.
(7) Obataya, I.; Kotaki, T.; Sakamoto, S.; Ueno, A.; Mihara, H. *Bioorg. Med. Chem. Lett.* **2000**, *10*, 2719−2722.
(8) Robertson, D. E.; Farid, R. S.; Moser, C. C.; Urbauer, J. L.; Mulholland, S. E.; Pidikiti, R.; Lear, J. D.; Wand, A. J.; DeGrado, W. F.; Dutton, P. L. *Nature* **1994**, *368*, 425−432.
(9) Shifman, J. M.; Gibney, B. R.; Sharp, R. E.; Dutton, P. L. *Biochemistry* **2000**, *39*, 14813−14821.
(10) Gibney, B. R.; Huang, S. S.; Skalicky, J. J.; Fuentes, E. J.; Wand, A. J.; Dutton, P. L. *Biochemistry* **2001**, *40*, 10550−10561.
(11) Ghirlanda, G.; Osyczka, A.; Liu, W.; Antolovich, M.; Smith, K. M.; Dutton, P. L.; Wand, A. J.; DeGrado, W. F. *J. Am. Chem. Soc.* **2004**, *126*, 8141−8147.
(12) Sakamoto, S.; Ueno, A.; Mihara, H. *Chem. Commun.* **1998**, 1073−1074.
(13) Sakamoto, S.; Obataya, I.; Ueno, A.; Mihara, H. *J. Chem. Soc., Perkin Trans. 2* **1999**, 2059−2069.
(14) Rosenblatt, M. M.; Huffman, D. L.; Wang, X.; Remmer, H. A.; Suslick, K. S. *J. Am. Chem. Soc.* **2002**, *124*, 12394−12395.
(15) Huffman, D. L.; Suslick, K. S. *Inorg. Chem.* **2000**, *39*, 5418−5419.
(16) Liu, D. L.; Williamson, D. A.; Kennedy, M. L.; Williams, T. D.; Morton, M. M.; Benson, D. R. *J. Am. Chem. Soc.* **1998**, *121*, 11798.
(17) Benson, D. R.; Hart, B. R.; Zhou, X.; Doughty, M. B. *J. Am. Chem. Soc.* **1995**, *117*, 8502.
(18) Nastri, F.; Lombardi, A.; Morelli, G.; Maglio, O.; DAuria, G.; Pedone, C.; Pavone, V. *Chem.—Eur. J.* **1997**, *3*, 340−349.
(19) Lombardi, A.; Nastri, F.; Marasco, D.; Maglio, O.; De, Sanctis, G.; Sinibaldi, F.; Santucci, R.; Coletta, M.; Pavone, V. *Chemistry* **2003**, *9*, 5643−5654.
(20) Arai, T.; Tsukuni, A.; Kawazu, K.; Aoi, H.; Hamada, T.; Nishino, N. *J. Chem. Soc., Perkin Trans. 2* **2000**, 1381−1390.
(21) Arai, T.; Kobata, K.; Mihara, H.; Fujimoto, T.; Nishino, N. *Bull. Chem. Soc. Jpn.* **1995**, *68*, 1989−1998.
(22) Akerfeldt, K. S.; Kim, R. M.; Camac, D.; Groves, J. T.; Lear, J. D.; Degrado, W. F. *J. Am. Chem. Soc.* **1992**, *114*, 9656−9657.
(23) Discher, B. M.; Koder, R. L.; Moser, C. C.; Dutton, P. L. *Curr. Opin. Chem. Biol.* **2003**, *7*, 741−748.
(24) Discher, B. M.; Noy, D.; Strzalka, J.; Ye, S.; Moser, C. C.; Lear, J. D.; Blasie, J. K.; Dutton, P. L. *Biochemistry* **2005**, *44*, 12329−12343.
(25) Ubarretxena-Belandia, I.; Engelman, D. M. *Curr. Opin. Struct. Biol.* **2001**, *11*, 370−376.
(26) DeGrado, W. F.; Gratkowski, H.; Lear, J. D. *Protein Sci.* **2003**, *12*, 647−665.

10.1021/ja057495i CCC: $37.00

elements into a predefined nativelike tertiary structure in membrane proteins are not completely understood.[25,26] Two distinct approaches have been used to circumvent these challenges in transmembrane four-helix bundles: in one approach, the bundle is stabilized via covalent attachment to a porphyrin template.[20−22] More recently, this problem has been addressed with amphiphilic maquettes that merge a transmembrane domain, derived from helix *d* of cytochrome bc_1, with a hydrophilic domain formed by a water-soluble, heme binding maquette; two members of this family, AP2 and AP3, bind heme in the transmembrane domain.[23,24]

Here, we present a simple model membrane hemoprotein, ME1, in which the cofactor is sandwiched between two transmembrane helices; the protein assumes a defined tertiary structure in both its *apo* and heme-bound state. The design is based on a well-established method to engineer novel functional proteins by grafting a non-native active site, in our case heme, into an existing inert protein.[27−35] Our choice of scaffold fell on glycophorin A (GpA), a small membrane protein that forms noncovalent dimers by the association of its single-helix membrane-spanning domain. GpA has been extensively characterized by mutagenesis,[36] analytical ultracentrifugation,[37,38] and NMR,[39,40] becoming a model system to study helix−helix interactions and association in membrane proteins. On this scaffold we mutated a limited number of residues in order to accommodate heme; the resulting sequence, ME1, displays the hallmarks of a functional membrane hemoprotein.

Results and Discussion

Design. The solution structure of the transmembrane domain of Glycophorin A[41] in dodecyl phosphocholine (DPC) micelles reveals a symmetric dimer in which two membrane-spanning α-helices cross at an angle of −40°, causing them to pack against each other at the N terminus and to diverge at the C terminus, forming a hydrophobic pocket that is still embedded in the transmembrane domain. Seven noncontiguous residues at the N terminus contribute to the noncovalent association interface and form the dimerization motif, LIxxGVxxGVxxT, as elucidated first by extensive mutagenesis studies[37,42,43] and confirmed later by the NMR structure.[41] In particular, the two glycines allow for an unusually close packing of the two helices and are necessary for dimerization.

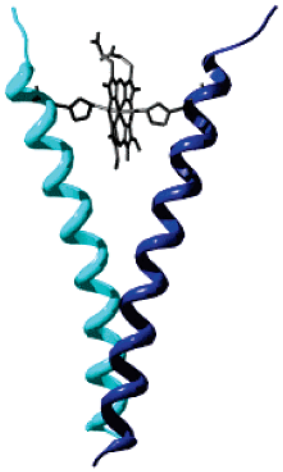

GpA: EPEITLIIFGVMAGVIGTILLISYGIRRLIKK
ME1: SPEIALIIFGVMAGVIGTILLASYGHRRLRKK

Figure 1. Ribbon model of ME1 in complex with hemin; the side chains of His 26, which provide the axial ligand for the iron center, are shown as sticks. The amino acid sequence of the transmembrane portion of glycophorin A is compared with ME1, and the five amino acids changed are highlighted in red.

Starting from the coordinates of GpA, we built a model of ME1 as described in Materials and Methods; briefly, the two helices were trimmed to the transmembrane region, eliminating the first eight residues, which lie outside the predicted transmembrane portion and are disordered in the structure. A heme-binding site was created in the cavity by mutating Ile 26 to His, which will provide the axial ligand for the heme group. Next, a heme group was manually placed into the cavity, oriented with its propionate groups facing the water-accessible extremity of the pocket (Figure 1). The side chain conformation of the coordinating histidines was modeled after those found in the heme binding site of cytochrome bc_1, placing the ϵ-nitrogens within binding distance from the porphyrin iron; this coordination mode is favored by the majority of natural heme-binding proteins.[11,44] In addition, two residues were modified to optimize the interactions between the protein and the prosthetic group: Ile 22 was changed to Ala to reduce steric clashes with the porphyrin ring, and Ile 30 (at the carboxyl terminus) was changed to Arg to introduce favorable electrostatic interactions with the propionates on the porphyrin ring. A Glu to Ser mutation for the first helical residue introduces an N-capping motif that stabilizes the N terminus. The side chain orientations of the newly introduced residues were manually optimized. The final sequence, ME1, contains five mutations out of the 32 amino acids in the sequence of the transmembrane segment of GpA (Figure 1); the residues comprising the dimerization interface were not affected by the mutations.

Binding of Hemin. ME1, reconstituted in DPC micelles, binds strongly to hemin; evidence for binding to the ferric and ferrous form is shown by UV−vis spectroscopy (Figure 2). After addition of a stoichiometric amount of ferric hemin to a solution of ME1 in DPC at pH 7.5, the absorbance spectrum is dominated

(27) Wilson, J. R.; Caruana, D. J.; Gilardi, G. *Chem. Commun.* **2003**, 356−357.
(28) Qi, D.; Tann, C. M.; Haring, D.; Distefano, M. D. *Chem. Rev.* **2001**, *101*, 3081−3111.
(29) Tann, C. M.; Qi, D.; Distefano, M. D. *Curr. Opin. Chem. Biol.* **2001**, *5*, 696−704.
(30) Levine, H. L.; Nakagawa, Y.; Kaiser, E. T. *Biochem. Biophys. Res. Commun.* **1977**, *76*, 64−70.
(31) Lu, Y.; Valentine, J. S. *Curr. Opin. Struct. Biol.* **1997**, *7*, 495−500.
(32) Lu, Y.; Berry, S. M.; Pfister, T. D. *Chem. Rev* .**2001**, *101*, 3047−3080.
(33) Hellinga, H. W. *Curr. Biol.* **1998**, *3*, R1−R8.
(34) Benson, D. E.; Wisz, M. S.; Hellinga, H. W. *Proc. Natl. Acad. Sci. U.S.A.* **2000**, *97*, 6292−6297.
(35) Dwyer, M. A.; Looger, L. L.; Hellinga, H. W. *Science* **2004**, *304*, 1967−1971.
(36) Lemmon, M. A.; Flanagan, J. M.; Treutlein, H. R.; Zhang, J.; Engelman, D. M. *Biochemistry* **1992**, *31*, 12719−12725.
(37) Fleming, K. G.; Ackerman, A. L.; Engelman, D. M. *J. Mol. Biol.* **1997**, *272*, 266−275.
(38) Fleming, K. G.; Engelman, D. M. *Proc. Natl. Acad. Sci. U.S.A* **2001**, *98*, 14340−14344.
(39) Smith, S. O.; Song, D.; Shekar, S.; Groesbeek, M.; Ziliox, M.; Aimoto, S. *Biochemistry* **2001**, *40*, 6553−6558.
(40) MacKenzie, K. R.; Prestegard, J. H.; Engelman, D. M. *J. Biomol. NMR* **1996**, *7*, 256−260.
(41) MacKenzie, K. R.; Prestegard, J. H.; Engelman, D. M. *Science* **1997**, *276*, 131−133.
(42) Lemmon, M. A.; Flanagan, J. M.; Hunt, J. F.; Adair, B. D.; Bormann, B. J.; Dempsey, C. E.; Engelman, D. M. *J. Biol. Chem.* **1992**, *267*, 7683−7689.
(43) Russ, W. P.; Engelman, D. M. *J. Mol. Biol.* **2000**, *296*, 911−919.
(44) Huang, S. S.; Koder, R. L.; Lewis, M.; Wand, A. J.; Dutton, P. L. *Proc. Natl. Acad. Sci. U.S.A.* **2004**, *101*, 5536−5541.

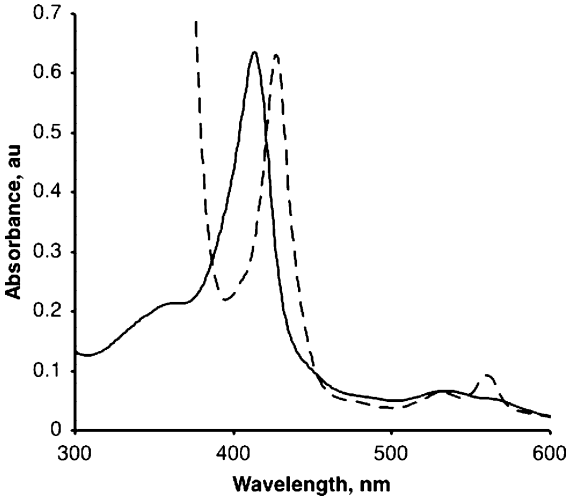

Figure 2. Absorbance spectra of ME1−hemin complex (solid line), [ME1] = 10 μM and porphyrin = 4.5 μM in DPC 2 mM, showing a strong Soret band at 413 nm and less distinct Q bands between 500 and 600 nm. Reduction of the complex upon addition of dithionite (broken line) results in a shift of the Soret band to 427 nm and in well-resolved Q bands at 530 and 560 nm.

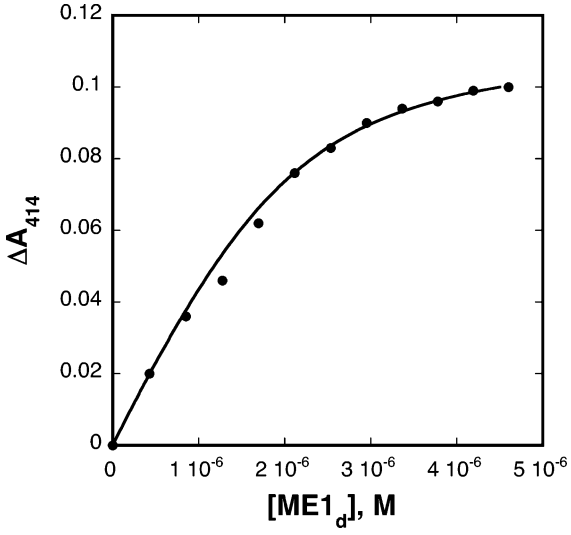

Figure 3. Hemin binding isotherm: the increase in absorbance at 414 nm obtained by titrating peptide into a 2 μM solution of hemin in 1.2 mM DPC, phosphate buffer, pH 7.2 is reported (●, experimental data) together with the fit obtained using a 1:1 binding model (eq 1). The peptide concentrations reported, in the 0 to 5 μM range, refer to the concentration of dimeric ME1.

by a strong Soret band at 414 nm and by weaker, less distinct α and β bands between 500 and 600 nm. The reduction of the complex to its ferrous form by addition of dithionite resulted in a marked red shift of the Soret band to 427 nm and the resolution of the broad Q bands into two distinct components at 530 and 560 nm, respectively. These values are consistent with bis-histidine ligation of the ferric and ferrous heme.[4,45] Control experiments showed that GpA, reconstituted in DPC micelles in similar conditions, does not bind hemin.

The apparent dissociation constant for binding of ME1 to ferric protoporphirin IX was determined by titrating peptide from a concentrated stock solution into a 2 μM solution of hemin in PBS containing 1.1 mM DPC. The formation of the complex was monitored at the Soret maximum of 413 nm. The binding isotherm obtained (Figure 3) was analyzed using a mutually depleting model in which one hemin binds to a preformed dimer, described in detail in the Materials and Methods section. The 2:1 peptide/hemin stoichiometry was confirmed independently by equilibrium sedimentation analysis. This model assumes that the peptide is fully dimeric in the concentration range examined and is supported by further experiments indicating that the mutations introduced in GpA do not alter its aggregation state (see next section). The equation derived from this binding model yields an apparent dissociation constant, $K_{d,app}$, of $(4.7 \pm 1.2) \times 10^{-7}$ M. For comparison, water soluble four-helix bundles bind two hemins with dissociation constants in the low nanomolar and low micromolar range, respectively, for the first and the second hemin;[4,10,46,47] amphiphilic four-helix bundles with one binding site within the lipophilic portion have apparent dissociation constants in the 50 to 450 nM range.[24] Simpler, covalently preorganized cyclic and hairpin peptides are in the low μM range.[48] The apparent dissociation constant determined for ME1 compares well with these systems.

Peptide Aggregation States: Apo ME1 was directly compared with the transmembrane domain of Glycophorin A by SDS-PAGE (Figure 4a): while electrophoresis in the presence of SDS is denaturing for water-soluble proteins, it can preserve the native folded states of membrane proteins. This technique has been used for the rapid assessment of the oligomerization states of small transmembrane proteins[26,36,37,49−51] such as phospholamban, GpA, and a series of membrane soluble GCN4 analogues designed by the Engelman and DeGrado groups. At the conditions used, ME1 migrates to a position identical to that of GpA, showing that the mutations introduced in ME1 are compatible with dimer formation. The hemin-bound protein was not included in the experiment, because the prosthetic group is stripped from the complex under the experimental conditions.

The aggregation state of the ME1−Hemin complex in detergent micelles was more accurately measured by analytical ultracentrifugation sedimentation equilibrium experiments.[26,38,50,52,53] The sedimentation curves reported in Figure 4b were obtained at peptide loading concentrations of 20 μM in 10 mM DPC, monitoring at the Soret maximum absorbance (414 nm). The data were analyzed using a single-species model, resulting in an apparent molecular weight of 8300 ± 400 Da, consistent with a theoretical molecular weight of 8200 Da for the 2:1 peptide/hemin complex.

These data support the hypothesis that ME1 forms strong, noncovalent dimers in a membrane-mimetic environment, presumably through the same interface that mediates the dimerization of GpA. Moreover, binding of the cofactor does not affect the oligomerization state of ME1.

CD Spectroscopy: The secondary structure of ME1 in its apo and hemin-bound state was assessed by circular dichroism

(45) Walker, F. A. *Chem. Rev.* **2004**, *104*, 589−616.
(46) Gibney, B. R.; Rabanal, F.; Reddy, K. S.; Dutton, P. L. *Biochemistry* **1998**, *37*, 4635−4643.
(47) Moffet, D. A.; Foley, J.; Hecht, M. H. *Biophys. Chem.* **2003**, *105*, 231−239.
(48) Rosenblatt, M. M.; Wang, J.; Suslick, K. S. *Proc. Natl. Acad. Sci. U.S.A* **2003**, *100*, 13140−13145.
(49) Zhou, F. X.; Cocco, M. J.; Russ, W. P.; Brunger, A. T.; Engelman, D. M. *Nat. Struct. Biol.* **2000**, *7*, 154−160.
(50) Choma, C.; Gratkowski, H.; Lear, J. D.; DeGrado, W. F. *Nat. Struct. Biol.* **2000**, *7*, 161−166.
(51) Gratkowski, H.; Dai, Q. H.; Wand, A. J.; DeGrado, W. F.; Lear, J. D. *Biophys. J.* **2002**, *83*, 1613−1619.
(52) Tanford, C.; Reynolds, J. A. *Biochim. Biophys. Acta* **1976**, *457*, 133−170.
(53) Tanford, C.; Nozaki, Y.; Reynolds, J. A.; Makino, S. *Biochemistry* **1974**, *13*, 2369−2376.

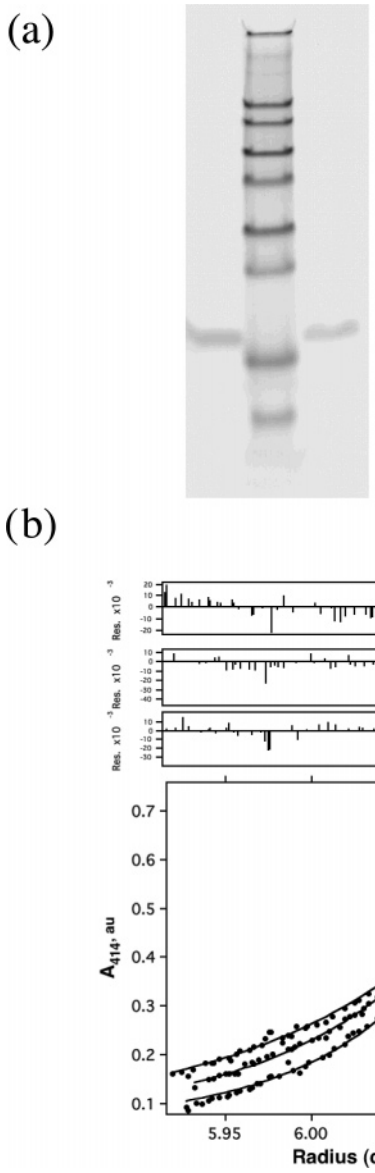

Figure 4. SDS-PAGE gel electrophoresis (a) of apo ME1 (right lane) compared with the transmembrane domain of GpA (left lane); water-soluble molecular markers are in the center lane. The two proteins migrate to the same position, corresponding to approximately 8000 Da, consistent with the formation of a dimer. Analytical ultracentrifugation sedimentation profile (b) for hemin-bound ME1; the data were analyzed using a single species model, yielding an apparent molecular mass of 8300 ± 400 Da. A global fit to three data sets, collected at 40 000, 45 000, and 50 000 K is shown. Conditions: peptide loading concentration 20 μM, 0.01 M sodium phosphate, pH 7.2, 0.05 M NaCl, and 10 mM DPC.

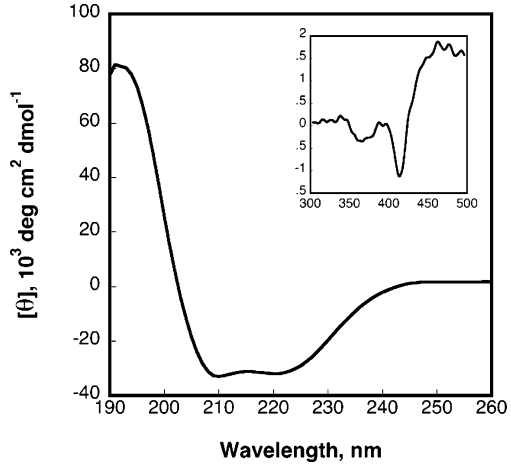

Figure 5. CD spectroscopy of ME1 in the presence of a stoichiometric amount of hemin; the spectrum was obtained at a peptide concentration of 11 μM in DPC 1.2 mM, potassium phosphate buffer 0.05 M, NaCl 0.1 M, pH 7.5. ME1 is highly helical (<95%) in the apo (not shown) as well as the hemin-bound state. The insert shows the induced dichroic signal observed in the visible part of the spectrum, corresponding to the Soret band of the hemin complex.

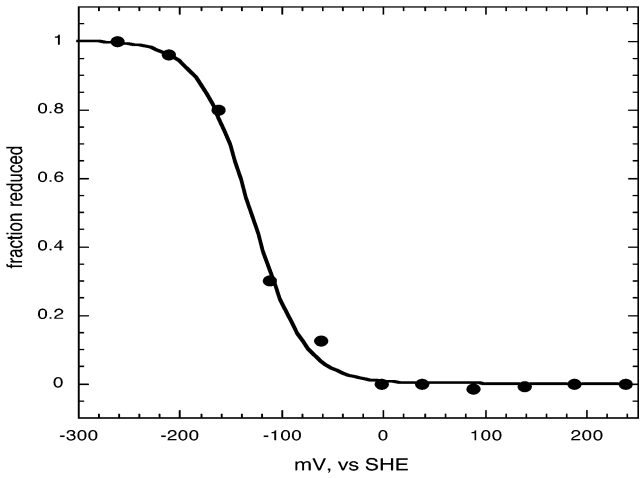

Figure 6. Potentiometric titration of ME1−hemin. Δ*A* values at 560 nm versus ambient potential in the 250 mV to −300 mV vs SHE were collected using a home-built cell, which uses a gold mesh working electrode, a Pt counter electrode, and an SCE reference electrode; the sample is dissolved at high concentration (see Materials and Methods) in DPC 20 mM, phosphate buffer 0.1 M, pH 7.2. The Δ*A* values were fraction reduced and analyzed using the Nernst equation for a one-electron couple, obtaining a midpoint equilibrium redox potential of −128 ± 2 mV vs SHE.

(Figure 5). The spectra obtained at a low micromolar concentration in DPC micelles are typical of the α-helical structure, showing characteristic minima at 208 and 222 nm; the mean residue molar ellipticity at 222 nm indicates that the peptides are more than 95% helical at room temperature. Such a high helical content is typical of transmembrane helical proteins and reflects the stabilization of interhelix backbone hydrogen bonds within the membrane.[26,54,55] The mutations made to wt GpA appear to be well tolerated and do not result in disruption of its secondary structure. Moreover, the absence of visible changes in secondary structure upon binding to hemin indicates that the peptide scaffold is preorganized, and folding does not depend on complex formation. The spectrum of the hemin-bound ME1 shows an induced dichroic signal in the Soret band region, indicating that the hemin experiences a chiral environment.[10,17,56]

Redox Potentiometry. The equilibrium midpoint potential of ME1−Hemin was determined by monitoring the difference in absorbance at the α band between the reduced and the fully oxidized species as a function of the ambient redox potential.[57] The resulting curve (Figure 6) analyzed according to the Nernst equation yielded a redox potential of −128 ± 3 mV vs SHE; this value is significantly more positive than those observed for bis-imidazole ligated hemin groups in hydrophilic environ-

(54) Popot, J. L.; Engelman, D. M. *Annu. Rev. Biochem.* **2000**, *69*, 881−922.
(55) White, S. H.; Wimley, W. C. *Annu. Rev. Biophys. Biomol. Struct.* **1999**, *28*, 319−365.
(56) Myer, Y. P.; Pande, A. In *The Porphyrins*; Dolphin, D., Ed.; Academic Press: New York, 1978; pp 271−322.
(57) Dutton, P. L. *Methods Enzymol.* **1978**, *54*, 411−435.

Table 1. Reduction Potential Values of Iron Porphyrins in Model Heme Protein Assemblies

Protein	Porphyrin reduction potential, mV vs SHE
Cytochrome bc_1[59]	30 to 70 (b_H) −50 to −120 (b_L)
Four-Helix Bundles	
Maquettes[10]	−150 to −220
Hecht library[47]	−110 to −170
D2-Heme[11]	−124
TASP-assembled[2]	−90 to −150
Rop-type[27]	−154
Amphiphilic Maquettes[a,24,60]	AP1 (C_8E_5 micelles) −90; AP1 (vescicles) −175 mV; AP2 (beta-OG) −125
Two-Helix Systems	
Sandwiched mesoheme[61]	−281 (Ala); −337 (Trp)
Mimochrome IV[b,19]	−80
Hairpin-Coproporphyrin[14]	−215 to −252
ME[1]	−128

[a] In AP1, the heme binding domain resides in the water-soluble portion of the maquette. [b] The unusually high reduction potential obtained for Mimochrome IV might be due to the experimental conditions used (tributylmethyl phosphonium chloride (TBMPC) membrane entrapping mimochrome IV and supported on graphite electrode) (V. Pavone, personal communication).

ments, typically around −220 mV vs SHE.[10] In comparison with water-soluble hemin-binding model proteins with bis-His ligation (Table 1), ME1 is at the high end of the spectrum. If compared to natural membrane proteins, ME1 is at the low end of the spectrum: in *Rhodobacter capsulatus* cytochrome bc_1 the two b-type hemes, b_H and b_L, have redox potentials of 40 and −110 mV, respectively.[58] Depending on species, these values can vary between 30 and 70 mV for b_H and between −50 and −120 mV for b_L.[59]

The redox potential of ME1 is significantly less negative than the values observed for water-soluble two-helix peptide−heme assemblies (Table 1). A value of −128 mV is consistent with the designed location of the heme, in a hydrophobic cavity but at the relatively more polar C-terminus of the transmembrane helix, which presumably will be close to the surface of the micelle; note also that the negatively charged propionate groups were designed to project toward the aqueous Stokes layer. The relationship between hydrophobic environment and redox potential of the heme is complex,[10,61] as it must factor in the difference in binding affinity in the oxidized and reduced states, as well as the possible effect of local electrostatic interactions due to the positively charged amino acids surrounding the heme in ME1. Further studies on ME1 mutants will allow us to dissect these factors.

Catalytic Activity. ME1 is able to catalyze the peroxide-dependent oxidation of organic substrates. This activity was characterized using as reducing agent 2,2′,5,5′-tetramethylbenzidine (TMB), which undergoes two successive one-electron oxidations in the presence of peroxide.[55] The time course of the reaction in the presence of low micromolar concentrations

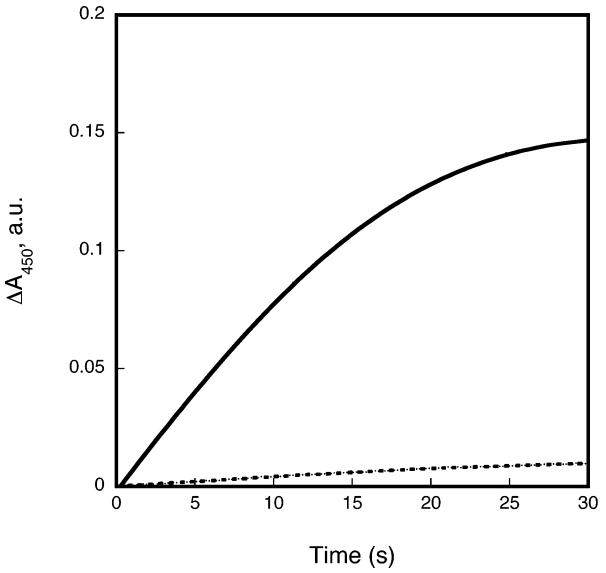

Figure 7. Time course of TMB oxidation in the presence of ME1−Hemin (continuous line) and hemin (broken line). Conditions: hemin concentration 2 μM, or [ME1−Hemin] 1.3 μM (calculated according to eq 1 from 2 μM hemin and 4 μM peptide) in phosphate 0.05 M, pH 7.5 containing 1.5 mM DPC, [H_2O_2] 6 mM, and 10 μM TMB.

of the ME1−Hemin complex or of micelle-solubilized hemin,[66,67] monitored by following the formation of TMB-ox at 450 nm, is reported in Figure 7. In these conditions, the reaction catalyzed by ME1−Hemin is about 20 times faster, as evaluated by initial velocities. The kinetic process was further analyzed by monitoring the reaction as a function of ME1−Hemin complex concentration. A plot of the corresponding initial velocities versus complex concentration, calculated according to eq 1 and the experimentally determined K_d, is linear in the 0−6 μM range (Supporting Information, Figure S1). An additional control experiment was aimed at determining the relationship between the formation of a 2:1 peptide/hemin complex and the observed catalytic activity. Thus, the reaction was monitored at constant hemin concentration and increasing peptide concentrations. The corresponding plot of initial velocities versus ME1 concentrations shows a steep increase at low peptides/hemin ratios, which reaches a plateau above the 2:1 ratio expected for ME1−Hemin complex formation (Supporting Information, Figure S2). Taken together, these data support the hypothesis that the observed catalytic activity requires the presence of a 2:1 ME1−Hemin complex.

A direct comparison with the peroxidase activity reported in previous studies[7,65] for water-soluble bis-histidine heme-binding model proteins is complicated by differences in conditions and cosubstrates explored. Perhaps the closest comparison is that with a library of heme-binding proteins described by Hecht.[65] In a preliminary screen, the proteins oxidized TMB with specific velocities, v_0/[Hemin], in the 500−1600 Abs_{450} s^{-1} M^{-1} range; in similar conditions, the value measured for ME1 is 2300

(58) Osyczka, A.; Moser, C. C.; Daldal, F.; Dutton, P. L. *Nature* **2004**, *427*, 607−612.
(59) Darrouzet, E.; Moser, C. C.; Dutton, P. L.; Daldal, F. *TiBS* **2001**, *26*, 445−451.
(60) Ye, S.; Discher, B. M.; Strzalka, J.; Xu, T.; Wu, S. P.; Noy, D.; Kuzmenko, I.; Gog, T.; Therien, M. J.; Dutton, P. L.; Blasie, J. K. *Nano Lett.* **2005**, *5*, 1658−1667.
(61) Kennedy, M. L.; Silchenko, S.; Houndonougbo, N.; Gibney, B. R.; Dutton, P. L.; Rodgers, K. R.; Benson, D. R. *J. Am. Chem. Soc.* **2001**, *123*, 4635−4636.
(62) Dunford, H. B. In *Peroxidases in Chemistry and Biology;* Everse, J., Everse, K. E., Grisham, M. B., Eds.; CRC Press: Boca Raton, FL, 1991; Vol. II, pp 1−24.
(63) Marquez, L. A.; Dunford, H. B. *Biochemistry* **1997**, *36*, 9349−9355.
(64) Dunford, H. B. *Heme Peroxidases;* John Wiley and Sons, Inc: New York, 1999.
(65) Moffet, D. A.; Certain, L. K.; Smith, A. J.; Kessel, A. J.; Beckwith, K. A.; Hecht, M. H. *J. Am. Chem. Soc.* **2000**, *122*, 7612−7613.
(66) Simplicio, J.; Schwenzer, K. *Biochemistry* **1973**, *12*, 1923−1929.
(67) Simplicio, J. *Biochemistry* **1972**, *11*, 2525−2528.

$Abs_{450}\ s^{-1}\ M^{-1}$. Based on this comparison, ME1 is slightly faster than Protein 86, the best performer in the library.

Conclusions

The modeling and experimental results described here demonstrate that it is possible to engineer a functional membrane protein by grafting a heme-binding site into an inert membrane protein, glycophorin A. This scaffold is particularly tolerant of mutations at its C-terminus, as the two helices diverge and define a hydrophobic cavity that is still embedded in the membrane environment. The protein obtained by introducing a bis-histidine binding site in the cavity, ME1, binds hemin with high affinity and maintains the same secondary structure and oligomerization state as wild-type GpA in both the *apo* and hemin-bound state. The midpoint reduction potential is within the range expected for a hydrophobic hemin environment. Although the heme-binding site was optimized for tight binding and not for catalysis, ME1 shows significant peroxidase-like activity.

Future studies with ME1 will be aimed at determining how mutations in the heme-binding cavity affect the binding affinity, midpoint reduction potential, and catalytic activity of ME1 variants, with the long-term goal of establishing rules for the de novo design of functional membrane proteins. These studies will be extended to binding of natural and unnatural cofactors.

Materials and Methods

Design. The NMR structure of glycophorin A[41] (PDB entry: 1AFO) in DPC micelles serves as the starting point for the design. A close examination of the structure in InsightII (Accelrys, Inc) identified unstructured residues at the N and C termini, which were trimmed. The shortened sequence was renumbered from 1 to 32. Residue Ile 26 in each helix, which points toward the center of the cavity, was manually changed to His. The heme was positioned with the heme iron atom at the midpoint between the Cα's of the two His residues and oriented with its propionate groups pointing toward the C-termini of the two helices. Additional substitutions were the following: Glu 1 to Ser, Thr 5 to Ala, Ile 22 to Ala, and Ile 30 to Arg. For each residue, the optimal rotamer was selected from the Insight library; thus, Ser 1 forms an N capping motif, His 26 coordinates the iron atom through its Nϵ, and Arg 30 makes electrostatic contacts with the heme propionate groups. Finally, the model was minimized with the Discover 3 module using the esff forcefield.

Materials. Fmoc-protected amino acids (Fmoc: 9-fluorenylmethoxycarbonyl), PAL resin (PAL: 5[4-(aminomethyl)-3,5-bis(methoxy)-phenoxy]valeric acid), HOBt (*N*-hydroxy benzotriazole), HATU (*N*-[9-dimethylamino-0-1*H*-1,2,3-triazolo[4,5-*b*]pyridino-1-ylmethylene]-*N*-methylmethan-aminium hexafluorophosphate) were purchased from NovaBiochem. All solvents and chemicals used in the peptide synthesis and purification were of the highest available grade and were used without further purification. Hemin (Fe(III)-Protoporphyrin IX) was purchased from Frontier Scientific.

Synthesis. The peptides were synthesized with standard solid-phase procedures on a Millipore 9050 synthesizer (PE Applied Biosystems) using XAL PEG-PS resin, cleaved according to standard Novabiochem protocols and purified by reversed-phase HPLC on a semipreparative C4 column (Vydac). All peptides were acetylated at the amino terminus. The peptides were determined to be at least 95% pure by analytical HPLC; MALDI-TOF analysis confirmed the expected molecular weight and purity.

Determination of Aggregation State. Sedimentation equilibrium analysis was performed using a Beckman XLI analytical ultracentrifuge. Initial peptide concentrations were 20 μM in 0.01 M sodium phosphate, pH 7.2, 0.05 M NaCl and 10 mM DPC; the density matching of the buffer to the DPC micelles was obtained at approximately 52% D_2O.[37,53,69] The samples were centrifuged at 40 000, 45 000, and 50 000 rpm; equilibrium was determined when successive interference radial scans at the same speed were indistinguishable. Interference fringe data and absorbance data at 280 and 414 nm were collected. Partial specific volume and peptide molecular mass were computed using the program SEDNTERP and corrected for deuterium exchange.[70]

The data were analyzed using a single-species model; curve fitting was performed using custom procedures on Igor Pro (WaveMetrics, Inc.).

SDS-PAGE analysis was carried out using a precast 10−20% gradient NOVEX Tricine minigel and commercial running and loading buffers (4% SDS and 1% SDS Tricine buffer, pH 8.3, respectively) in an XCell Surelock minicell connected to a PowerEase 500 power supply. The gel was stained with Coomassie Brilliant Blue for visualization. Supplies and equipments were purchased from Invitrogen.

Redox Titrations. Chemical oxidation−reduction midpoint potential titrations of purified complexes were performed using a home-built cell, which uses a gold mesh (333 lines/inch, Buckbee-Mears, Inc) working electrode and a Pt counter electrode; an SCE reference electrode is connected to the cell via a salt bridge containing 60 mM KCl. The grid was prepared by treatment with a solution containing 11 mg of Aldrithiol (4,4 dipyridyl disulfide, Aldrich) in 50 mL of 0.2 M Tris-HCl, pH 8, at room temperature for about 2 h, and rinsed thoroughly with ddH_2O. The ME1−Hemin complex prepared in 20 mM DPC, PBS buffer, pH 7.2 was concentrated in a Centricon-100 to an absorbance A_{800} of about 60 and a volume of 10 μL. To this sample were added the following redox mediators: potassium ferro/ferricyanide; 2,3,5,6-tetramethyl-1,4-phenylenediamine; duroquinone; pyocyanine; anthraquinone-2,6-disulfonate; and benzyl viologen at concentrations of 15−30 μM. The sample is deposited directly on the grid, and the cell is assembled by packing two quartz windows, separated by an O ring, against the grid. Both the sample and the perimeter solution were adjusted to a KCl concentration of 60 mM. The redox potential of the sample was poised over the range −300 mV to +200 mV in 50 mV intervals with a potentiostat (Bioanalytical Systems Voltammograph CV-370) and the voltage read after a 10 min equilibration time. The optical changes (in the region 500−600 nm) that accompanied redox potential change were recorded on a modified Cary 500 (Varian). The E_m values were determined by fitting the data to a single $n = 1$ Nernst expression.

CD Measurements. CD spectroscopy was carried out at 25 °C using a J-710 spectropolarimeter (Jasco). The samples were prepared in 0.02 M potassium phosphate buffer pH 7.2 containing NaCl 0.1 M and DPC 2 mM; the apo peptide concentration was 20 μM, to which 10 μM hemin from a concentrated stock in KOH 0.1% was added. A quartz cell with a 1 mm path length was used for the measurements.

Binding Affinity. The binding affinity of the peptide for hemin was evaluated by titrating increasing amounts of peptide into a solution containing 2 μM hemin in PBS buffer, DPC 1.1 mM, to total peptide concentrations in the 0 to 8 μM range. Complex formation was monitored by monitoring the Soret band at 414 nm for each peptide concentration, after a 5 min equilibration time. The binding curve obtained by plotting the absorbance at 414 nm vs the peptide concentration was analyzed according to the following mutually depleting binding model, which assumes that all the peptide will be in dimeric form at the concentrations used. If the K_{Dim} of 0.16 μM obtained by FRET for the transmembrane portion of glycophorin A in 25 mM DPC[71] is used as an approximation for ME1, the peptide is more than 85% dimeric at the low micromolar concentrations used. Note that the

(68) Mazumdar, S.; Springs, S. L.; McLendon, G. L. *Biophys. Chem.* **2003**, *105*, 263−268.
(69) Stouffer, A. L.; Nanda, V.; Lear, J. D.; DeGrado, W. F. *J. Mol. Biol.* **2005**, *347*, 169−179.
(70) Kochendoerfer, G. G.; Salom, D.; Lear, J. D.; Wilk-Orescan, R.; Kent, S. B.; DeGrado, W. F. *Biochemistry* **1999**, *38*, 11905−11913.
(71) Fisher, L. E.; Engelman, D. M.; Sturgis, J. N. *J. Mol. Biol.* **1999**, *293*, 639−651.

dimerization constant for GpA was determined at a molar excess of detergent of 150 000, whereas, at the lower DPC concentration used for the hemin titration experiment, the molar excess of detergent is about 300. The degree of dimerization depends sharply on the peptide/detergent ratio,[71] which is the relevant peptide concentration variable.[26]

$$P + P \rightleftarrows P_2$$

$$P_2 + H \rightleftarrows HP_2$$

where P represents ME1 (i.e., a single transmembrane helix), P_2 is the preformed dimer of apo ME1, H is hemin, and HP_2 is the cofactor-bound ME1.

The apparent dissociation constant can be derived as follows:

$$K_{d,app} = ([H_u][P_{2,f}])/[HP_2] \quad (1)$$

where $[H_u]$ is the concentration of the unbound hemin, $[P_{2,f}]$ is the concentration of the nonbound peptide, and $[HP_2]$ is the concentration of the complex formed.

The total hemin concentration, $[H_t]$, is equal to $[H_u] + [H_b]$, i.e., the sum of unbound and bound hemin, also expressed as $[HP_2]$. The total peptide concentration, $[P_{2,t}]$, is equal to the sum of free and bound peptide, i.e., $[HP_2]$. Thus,

$$K_{d,app} = ([H_t] - [H_b])([P_{2,t}] - [P_{2,b}])/[HP_2] = ([H_t] - [HP_2])([P_{2,t}] - [HP_2])/[HP_2]$$

The absorbance at 414 nm at zero peptide concentration is equal to

$$A_0 = \epsilon_u[H_u] = \epsilon_u[H_t]$$

At any peptide concentration, the total absorbance will be

$$A_t = \epsilon_u[H_u] + \epsilon_b[H_b] = \epsilon_u([H_t] - [H_b]) + \epsilon_b[H_b]$$

ϵ_u and ϵ_b are the extinction coefficients of the unbound and bound hemin, respectively. Thus, the change in absorbance at any given peptide concentration will be equal to

$$\Delta A_t = \Delta\epsilon[H_b],$$

where $\Delta\epsilon$ is the difference between the extinction coefficients of the bound and unbound hemin.

Substituting $[H_b]$ with $\Delta A_t/\Delta\epsilon$ and rearranging the terms of the equation,

$$K_d = (([H_t] - \Delta A_t/\Delta\epsilon)([P_{2,t}] - \Delta A_t/\Delta\epsilon))/\Delta A_t/\Delta\epsilon$$

The equation is solved for $[P_t]$, obtaining

$$[P_t] = ((\Delta A_t K_d)/(\Delta\epsilon[H_t] - \Delta A_t)) + \Delta A_t/\Delta\epsilon \quad (2)$$

Solving the equation for P_t instead of the more conventional ΔA_t, i.e., using a "reverse fitting" method, allows the use of closed form solution algebra and greatly simplifies the equation. The data were analyzed using KaleidaGraph (Synergy Software) according to eq 2; the error bars reported refer to the 95% confidence intervals.

The surfactant concentration is a crucial parameter in determining the binding affinity: increasing the DPC concentration to 5 mM resulted in a $K_{d,app}$ of $(6.4 \pm 0.2) \times 10^{-6}$ M, roughly 10-fold higher. This effect could be explained by the ability of the micellar detergent to solubilize hemin and compete with the peptide or by a shift in the peptide monomer−dimer equilibrium at higher DPC concentrations. Indeed, hemin has been shown to be monodisperse in surfactant micelles at high micromolar concentrations and at a wide range of pH.[66,67] Control experiments show that optimal incorporation is carried out at a lipid concentration around the cmc, which is 1.1 mM for DPC in phosphate buffer, pH 7; subsequent addition of surfactants to the preformed complex does not result in significant changes, as assessed by monitoring the absorbance at 413 nm over a period of 24 h.

Peroxidase Kinetics. Experiments were conducted in a reduced-volume quartz cuvette (1 cm path length); conditions: 4 μM ME1, 50 mM PBS pH 7, 2 μM hemin (from a stock in 100 mM KOH), 1.5 mM DPC, and 10 μM TMB (from a stock in 100% EtOH). The reaction was initiated by addition of HOOH to a final concentration ranging from 0.1 to 10 mM. The hydrogen peroxide stock concentration was standardized by UV−vis ($\epsilon_{230} = 72.8\ M^{-1}\ cm^{-1}$). TMB absorbs strongly at 450 nm upon two-electron oxidation (TMB-ox); the formation of a single-electron oxidation intermediate, $TMB^{\bullet+}$, can be monitored at 652 nm. The reaction was monitored at both wavelengths ($\epsilon_{652} = 39\,000\ M^{-1}\ cm^{-1}$, TMB intermediate and $\epsilon_{450} = 59\,000\ M^{-1}\ cm^{-1}$, final product, TMB_{ox})[63] using a Cary-50 UV−vis spectrometer. The initial velocities, υ_o, observed at 450 nm were plotted versus the increasing ME1−Hemin concentration, calculated according to eq 2, obtaining a linear correlation.

Control experiments with the hemin-catalyzed reaction were carried out at 2 μM hemin (from a stock in 100 mM KOH), 50 mM PBS pH 7, 1.5 mM DPC, and 10 μM TMB; the reaction was initiated by addition of hydrogen peroxide, as described above. In this case, the hemin is solubilized by the presence of the surfactant micelles.[66,67]

Acknowledgment. We thank the Protein Facility at ASU, in particular Dr. Dan Brune and Mr. John Lopez for assistance with the peptide synthesis and MALDI-TOF analysis, Dr. Joann Williams for the use of the home-built redox cell, Dr. Ira M. Bennett and Ms. Katie Alley for technical assistance, and Profs. Wilson Francisco and Edward Skibo, as well as members of the Ghirlanda lab for critical reading of the manuscript. This work was supported by NSF CAREER Award 0449842 to G.G. and by an NSF IGERT fellowship to J.M.C.

Supporting Information Available: Figure showing linear dependence of the observed initial velocities for the oxidation of TMB in the presence of ME1−Hemin and figure of initial velocities for the oxidation of TMB at constant hemin concentration as a function of [apo ME1] concentration. This material is available free of charge via the Internet at http://pubs.acs.org.

JA057495I